Interaction and diffusion of potassium on $Cr_2O_3(0001)/Cr(110)$

W. Zhao, G. Kerner, and M. Asscher*
Department of Physical Chemistry and the Farkas Center for Light Induced Processes, The Hebrew University, Jerusalem 91904, Israel

X. M. Wilde, K. Al-Shamery, and H.-J. Freund
The Fritz Haber Institute der Max-Planck Gesellschaft, Faradayweg 4-6, Berlin, Germany

V. Staemmler and M. Wieszbowska
Universität für Theoretical Chemie, Ruhr Universität Bochum, D-44780, Germany
(Received 24 March 1999; revised manuscript received 9 February 2000)

The interaction of potassium atoms on top of $Cr_2O_3(0001)/Cr(110)$ has been studied using work-function ($\Delta\Phi$), temperature programmed desorption (TPD), and optical second-harmonic generation (SHG) measurements. Potassium grows via the completion of a first layer, followed by a second layer in the form of two-dimensional (2D) islands, and at higher coverage 3D clusters are formed. This growth model is supported by and consistent with the results obtained from all three methods. Work-function data suggest that annealing at temperatures above 350 K results in the formation of a surface potassium oxide compound, provided the potassium coverage is higher than 0.5 monolayers (ML). Diffusion of alkali-metal atoms on an oxide surface is reported here over distances of several micrometers. This was measured using optical SH diffraction from coverage gratings that were generated by laser-induced thermal desorption. The activation energy for surface diffusion of potassium on $Cr_2O_3(0001)/Cr(110)$ has been determined to be 11 ± 0.5 kcal/mol with a preexponential factor $D_0=10^5$ cm^2/sec in the coverage range of 1.5–2.5 ML, dropping to 9 kcal/mol and $D_0=3\times10^3$ cm^2/sec at a coverage of 3.0 ML. These results are consistent with the diffusion of atoms in the third layer, on top of two-dimensional potassium islands in the second layer, the activation energy represent the barrier for descending from the 2D islands.

I. INTRODUCTION

The interaction of metal particles on oxide substrates has been the focus of increasing interest in recent years due to the extremely wide range of applications in which these systems play an important role.[1,2] In particular, geometric and electronic structure and the resulting chemistry of small metallic particles on oxide surfaces have been studied.[1–5] It is surprising to realize, however, that, despite the importance of oxides as support materials in catalysis, none of the studies so far have addressed the effect of ionic substrates, such as oxides, on the mechanism and rates of macroscopic diffusion as input for understanding sintering phenomena.

In contrast, adsorbate diffusion on well-defined metal surfaces has received growing experimental and theoretical attention over the last decade.[6,7] The introduction of laser desorption techniques has significantly increased the variety of atoms and molecules for which surface diffusion can be studied.[8–15] Of special interest is the diffusion of alkali metals, due to their well-known promotion effect in catalysis, and the dependence of this promotion effect on alkali-metal dispersion and coverage on the surface of the catalyst. One of the key questions that remains open for many of the alkali-metal–surface systems is the degree of charging or ionicity of the alkali metal and how it changes with coverage.

Numerous experimental techniques have provided information on alkali-metal surface-diffusion kinetics, from which activation energies for diffusion and preexponential factors have been obtained. In the limit of zero coverage, however, rather different numbers were reported, varying from 17.5 [K on W(112)],[16] to 2 kcal/mol [K on Pd(111), Na on Cu(100)].[17,18] Surface damage due to sputtering,[19] surface cleanliness,[20] and surface anisotropy[21] have all been shown to dramatically affect the surface diffusion of alkali metals. Diffusion by movement into the second layer,[22] the formation of islands,[23–26] and substitution into the lattice[27–29] have been postulated as possible reasons for the effect of coverage on diffusion.

Laser-induced thermal desorption (LITD) has been used to study the diffusion of potassium on clean Ru(001) as a function of surface coverage employing the hole-refilling method.[10] The LITD technique has also been employed to create a periodic coverage modulation of K on Re(001) (Ref. 30(a)] and Ru(001),[30(b)] from which diffusion can be measured using second-harmonic (SH) optical diffraction. this technique has provided valuable information in several other cases utilizing either second-harmonic[10,14,31–33] or linear diffraction,[12,14,34,35] both of which were demonstrated to be effective in monitoring diffusion on the length scale of micrometers. Monitoring diffusion using SH diffraction is especially effective for alkali metals due to their strong second-harmonic generation (SHG).[30]

In this study we present the results of our measurements addressing the effect of an ionic oxide substrate [$Cr_2O_3(0001)/Cr(110)$] on the interaction and also on the surface diffusion of potassium. The interactions of sodium[36(a)] and potassium[36(b),36(c)] with $Cr_2O_3(0001)$ have previously been investigated utilizing x-ray photoelectron spectroscopy (XPS) and laser desorption, while studying the photochemical response of the adsorbed potassium. Here we have employed TPD, work-function, and optical SH diffraction methods to study the adsorption and diffusion of potassium on chromium oxide. The formation of two-dimensional (2D) islands in the second layer and 3D clusters at higher coverages was identified by all three techniques. The barrier

 ©2000 The American Physical Society

for diffusion as it changes with coverage has been discussed in terms of the diffusion mechanism within the third layer.

II. EXPERIMENT

The details of the experimental apparatus[37,38] and the laser setup[15,30] were given elsewhere. Briefly, the experimental system is based on an UHV chamber with a base pressure below 8×10^{-11} Torr, equipped with a sputter gun, a quadrupole mass spectrometer (QMS), and a Kelvin probe. A *p*-polarized pulsed Nd:YAG (yttrium aluminum garnet) laser (Quantel YG585) at a fundamental wavelength of 1.064 μm, having a repetition rate of 10 Hz and pulse duration of 10 nsec (full width at half maximum), was used for both potassium coverage determination and the diffusion measurements. The laser pulse was split into two beams; the high-power beam was used for coverage grating formation via LITD, while the lower-power part was used as a probe beam. The probing technique was based on optical second-harmonic diffraction from the adsorbate grating. In the experiments reported here, the high-power pulse was split at a ratio of 1:1 for heating the surface and causing the necessary interference to form the monolayer grating. The two beams struck the potassium-covered $Cr_2O_3(0001)$ surface at incident angles of $\phi=\pm9.2°$ from the normal to the surface. These beams spatially overlapped at the center of the sample with a spot size of 0.34 cm^2. The maximum power density of the laser used for LITD actually absorbed by the sample per pulse (both beams) was approximately 11 MW/cm^2 (150 mJ/pulse). A spatial intensity modulation is formed under these conditions due to interference between the two beams. As a result, a periodic potassium coverage modulation is created in a gratinglike pattern.

The 1.064 μm probe laser hit the center of the sample at an incident angle of 45° from the normal to the surface with a spot size of 0.05 cm^2 to ensure that the probe laser fell within the area of grating formation. The absorbed fundamental laser intensity was at most 1.0 MW/cm^2, which corresponds to a maximum transient jump in surface temperature of 30 K; ensuring negligible diffusion of potassium due to and during the pulse of the probe laser.

The preparation and characterization of the $Cr_2O_3(0001)$ surface following oxidation of the clean Cr(110) metal surface were described elsewhere in detail.[36] Briefly, the cleaning procedure involved prolonged sputter-annealing cycles to eliminate any contaminants that can be detected by Auger spectroscopy. The oxidation procedure was then performed by exposing the clean metal at a temperature of 540 K for 1 min to oxygen at an ambient pressure of 2×10^{-6} mbar, then at 780 K for another 2 min, followed by annealing to 1000 K. Before each measurement, the sample was cleaned by flashing to 1000–1050 K under UHV conditions. The 3–4 nm thick oxide layer formed has the hexagonal (0001) plane exposed, as revealed and verified by low-energy electron diffraction (in a different UHV chamber). Temperature control and TPD measurements have been described elsewhere.[30] The chamber was equipped also with a Kelvin probe for work-function measurements, the probe can be operated in a $\Delta\Phi$-TPD mode.[39]

Potassium was dosed onto the $Cr_2O_3(0001)/Cr(110)$ surface by passing current (4.5–6.5 A) through a commercial potassium source (SAES Getters) located approximately 20 mm from the sample. This was sufficient to produce a monolayer (ML) of potassium on the surface within 2–3 min. Potassium surface coverages were generated by first exposing the oxide to ~3 ML of potassium atoms and subsequent annealing of the surface to a given temperature (approached at 3 K/sec) in the range 900–300 K. In this way, highly reproducible coverages could be obtained (within 5% of a monolayer) in the coverage range 0–2.5 ML, as determined and calibrated by integrated TPD peak-area measurements.[40]

III. RESULTS AND DISCUSSION

A. TPD of K from $Cr_2O_3(0001)/Cr(110)$

TPD spectra of potassium from the $Cr_2O_3(0001)$ surface reveal three distinct desorption peaks (heating rate of 10 K/sec, Fig. 1). A low-coverage desorption peak appears near 850 K, shifting to 600 K on completion of the first monolayer. Unlike the case of alkali-metal desorption from metallic substrates,[40(b)] the peak desorption temperature that pertains to a coverage of 1 ML is relatively high. This observation is consistent with the potassium atoms being partially positively ionized even at the completion of the first layer, unlike the complete neutrality believed to be the case when 1 ML is adsorbed on metallic surfaces.[30] The width of the TPD peak reflects the usual repulsive interactions between neighboring K adatoms. The effect of growing repulsion as coverage increases on the desorption spectra of alkali metals has been discussed in great detail in the literature, using various electrostatic models.[40] In our case—$K/Cr_2O_3(0001)$—an activation energy for desorption of 59 ± 5 kcal/mol has been obtained in the limit of zero coverage, assuming a ''standard'' preexponential factor of $10^{13}\,sec^{-1}$. This can be compared with the activation energy of 68.5 kcal/mol recently reported for the K/Re(001) system.[40(b)]

Above 1 ML, further decrease of the binding energy of potassium is observed as coverage increases. This can be explained by the same repulsive interactions between neighboring K adatoms. Since the $Cr_2O_3(0001)/Cr(110)$ surface is hexagonal, the density of potassium atoms on completion of the first layer is assumed to be similar to that observed on most metallic hexagonal surfaces (e.g., $K/Ru(001)=0.33$). This means a nearest K-neighbor separation for K atoms of 4.95 Å. K atoms in the second layer are expected to reside at sites slightly above the first-layer atoms, but still close enough to the underlying chromium ions of the substrate to have significant binding of these second-layer atoms to the surface. This explains the relatively high desorption temperature of the potassium atoms from this layer. The second peak at 450 K (binding energy of 27 ± 2 kcal/mol) is thus understood to correspond to desorption of potassium from 2D islands formed on top of the first monolayer. A measurable and reproducible desorption rate of potassium is also observed between 450 and 600 K. This is explained as the result of single adatoms on top of the completed first layer. The potassium coverage is clearly less than 2 ML when the first indication of a peak at 450 K appears. In fact, only when the clear onset of desorption from the third layer, or 3D islands, is observed at 360 K does the integrated TPD signal reach twice that found near 600 K, the full first monolayer signal. Finally, the multilayer potassium desorption peak, at

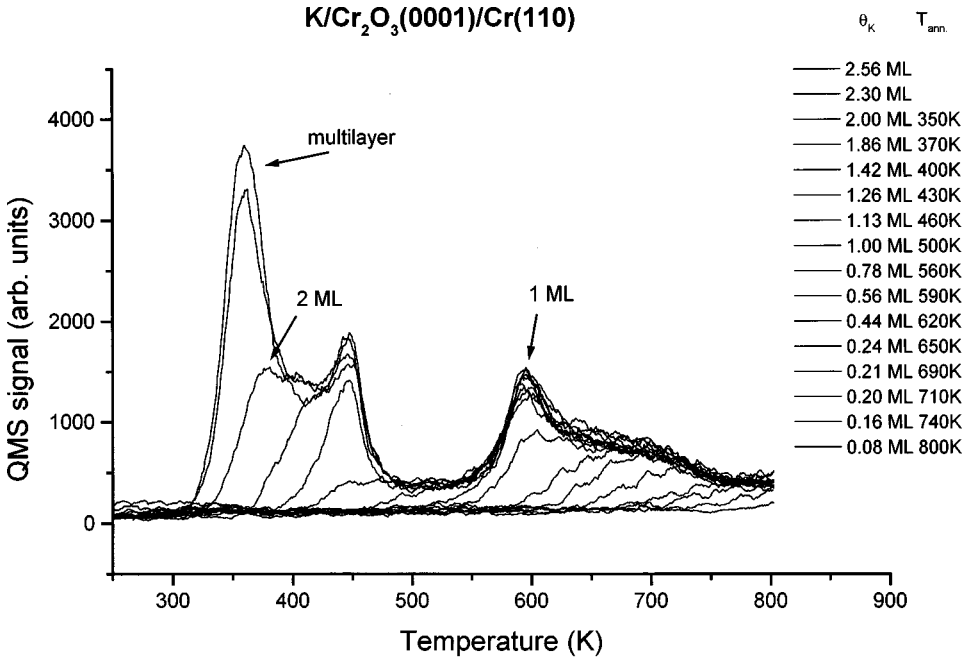

FIG. 1. TPD spectra of potassium from Cr_2O_3(0001)/Cr(110) at the indicated initial potassium coverages at a heating rate of 10 K/sec. To achieve the stated coverage, a multilayer of potassium is annealed (at 3 K/sec) to a specific temperature, as indicated.

360 K, is similar to that for multilayer potassium desorption from metallic substrates [Ru(0001) (Ref. 10) and Re(001) (Ref. 30).]

B. Work-function change measurements

Work-function change ($\Delta\Phi$) measurements for potassium on Cr_2O_3(0001)/Cr(110) as a function of the potassium coverage are depicted in Fig. 2, representing the average of three independent spectra taken on different days on freshly prepared oxide surfaces. The potassium coverage was prepared as described in Sec. III A above and Fig. 1. The curve of $\Delta\Phi$ vs coverage shown in Fig. 2 is similar but not identical to the one found in the case of alkali metals on metal surfaces.[40–43] It reaches its maximum negative value near 0.5 ML, here a decrease of 2.4 ± 0.3 eV, similar to the results reported previously on this system.[36(c)] The work-function increase of more than 1 V observed for coverages beyond 0.5 ML, however, is quite different from the earlier $\Delta\Phi$ spectra taken following potassium evaporation at 300 K (without annealing) where there is only a very small increase (0.2 V) above 0.5 ML.

The work-function increase in the case of alkali metals on metal substrates at coverages above 0.5 ML is discussed in the literature in terms of depolarization that arises from dipole-dipole repulsion among neighboring potassium adatoms.[40,42] This behavior on metals has been explained quantitatively as originating from the gradual growth of neutral alkali-metal islands as coverage increases, which coexist with isolated, partially ionized adsorbed atoms.[40,43] An alternative explanation is the gradual, coverage-dependent increase of the polarizability of the adsorbed alkali metal as coverage increases.[41]

It is necessary to explain the difference between the behavior of $\Delta\Phi$ vs coverage above 0.5 ML for the case of K on Cr_2O_3(0001)/Cr(110) given here following the annealing process and the curve reported previously without annealing[36c] and reproduced in this study. The very small

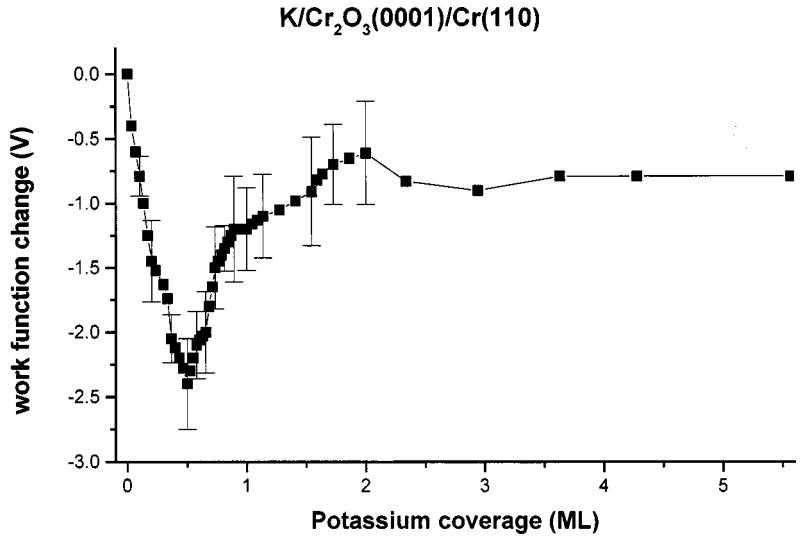

FIG. 2. Work-function change ($\Delta\Phi$) vs potassium coverage on Cr_2O_3(0001)/Cr(110). Potassium was deposited at a surface temperature of 300 K. The solid line is a guide for the eye.

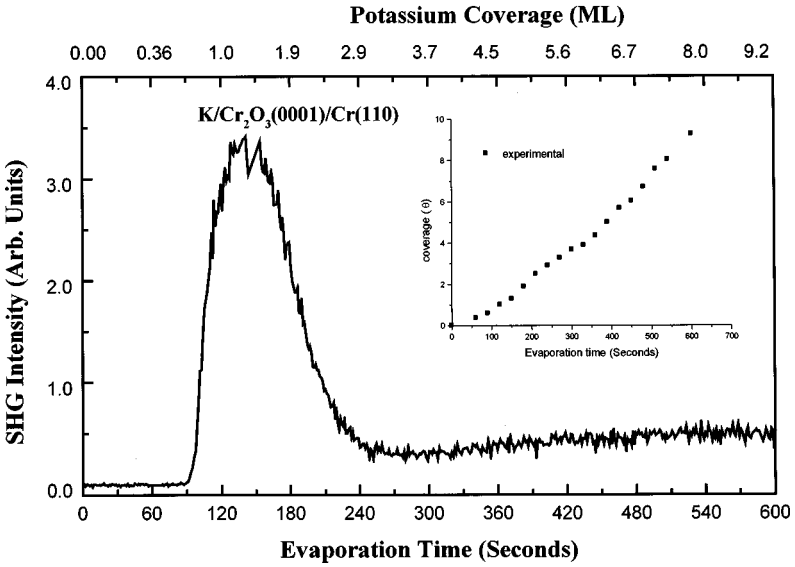

FIG. 3. SHG signal intensity recorded during potassium deposition on $Cr_2O_3(0001)/Cr(110)$ at 95 K.

work-function increase (compared to metal substrates) at coverages above 0.5 ML at 300 K without annealing[4,36(c)] could be related to the strongly ionic character of the alkali-metal layer which is retained all the way to completion of the first layer. This prevents the gradual development of metallic nature or depolarization at high coverage and therefore no significant change in the work function is observed above 0.5 ML. The strongly ionic character is supported by the unusually high desorption temperature of the potassium atoms on completion of the first layer (600 vs 350 K on clean metallic substrates; see Fig. 1). This is in contrast to the behavior on metallic substrates, where above 0.5 ML depolarization gradually increases the metallic character of alkali-metal adsorbates, thus leading to a significant turnover between 0.5 and 1.0 ML.

The curve shown in Fig. 2 following annealing of potassium on the oxide surface, however, represents a rather different process. The sharp increase in $\Delta\Phi$ above 0.5 ML is believed to be associated with the sudden, thermally activated formation/synthesis of a potassium oxide surface compound. The fact that this sudden turnover to a positive work-function change occurs only near 0.5 ML and not at lower coverages suggests that the stoichiometry of this compound (possibly K_2O) requires a minimum density of neighboring potassium atoms. The compound has to be oriented with the positive potassium ions closer to the oxide surface and the oxygen with its negative charge toward the vacuum side. In this way, the dipole direction leads to a work-function increase, as observed.

There is an interesting ''hump'' in the work-function change around the completion of the second monolayer following the annealing process, as seen in Fig. 2. This is a rather reproducible observation in spite of the relatively large error bars in this coverage range. It is not yet fully understood, but we tend to attribute this unique behavior (not found on metal substrates) to the growth of 2D and perhaps already the initial growth of 3D islands, as discussed in Sec. III A.

C. Optical SHG

Optical second-harmonic generation is a useful technique to monitor surface coverage of adsorbates during deposition or TPD. This is particularly so with alkali metals, for which the SH signal is very large.[40(b),44] In Fig. 3, the SH signal obtained during K evaporation onto $Cr_2O_3(0001)/Cr(110)$ at 95 K is shown after translating evaporation time to coverage, using the calibration curve in the inset of Fig. 3. We find the uncertainty level associated with evaporation time calibration to be $\pm 15\%$. It is evident that a broad maximum in the SH signal is obtained at coverages in the range 1.2–1.6 ML, with 1 ML defined as the first monolayer coverage based on the peak desorption temperatures as discussed above in Sec. III A. This maximum is found at higher coverage on the oxide than that previously reported for alkali metals on metal surfaces, where a pronounced peak has been observed near the completion of the first monolayer.[40(b),44] This different behavior is consistent with a slower conversion of the potassium layer on oxides into a fully metallic one, that is, at higher coverages.

Complementary information is obtained when the SHG signal is recorded during sample heating, following deposition of a well-defined initial coverage. Such SH-TPD spectra are shown in Fig. 4. These spectra reveal very clearly that above 650 K the SH signal is very weak, indicating that potassium atoms at these coverages on the oxide surface are rather ionic in nature. The SH-TPD spectra in Fig. 4 do not simply reproduce the actual desorption events as recorded by the mass spectrometer in Fig. 1. For initial coverages in the range 0.4–0.6 ML, there is a clear increase of the SH signal intensity in the temperature range between 150 and 300 K, before any desorption takes place (see Fig. 1). This can be attributed to structural rearrangements within the adsorbed layer on the surface, which lead to signal enhancement. In fact, as shown below, near 130 K surface diffusion is already significant. At higher coverages, just above 320 K, the SH-TPD spectra reveal the onset of two new peaks—a sharp one at 325 K and a broader peak at 390 K. The peak at 325 K shows up from initial coverages of 1.7 ML and becomes more intense as coverage increases. Above 3 ML, the SH-TPD spectra no longer change, except for small and slow changes at the baseline signal level due to plasmonic resonant effects at multilayer alkali-metal coverages, as has been discussed in the literature.[10(c)] The sharp peak near 325 K coincides with the appearance of 3D structures and multilay-

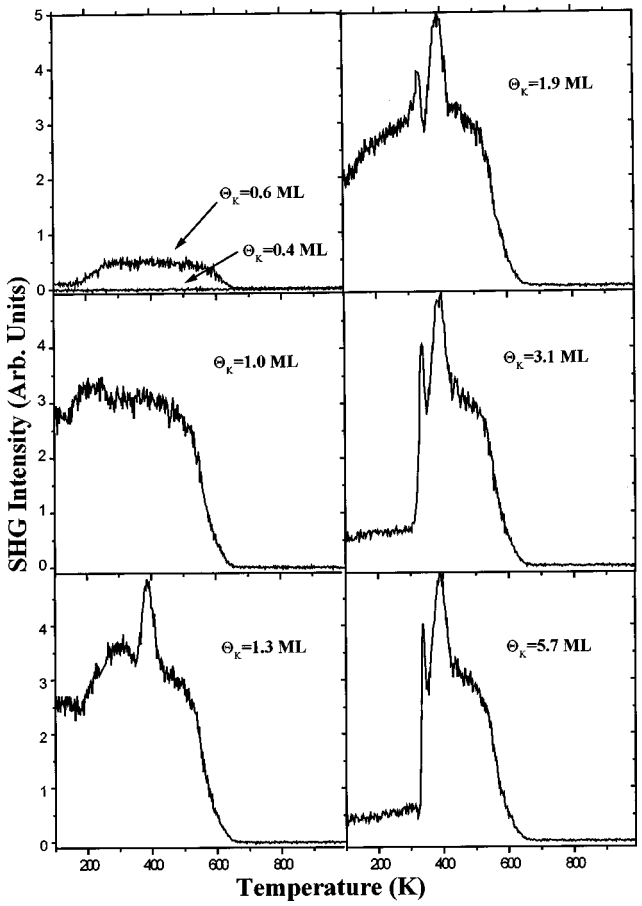

FIG. 4. SHG signal intensity recorded during TPD of potassium from Cr_2O_3(0001)/Cr(110) for the indicated initial potassium coverages. Heating rate is 6 K/sec and the deposition temperature is 95 K.

ers, just before their desorption from the surface. As seen in Fig. 1, the TPD spectra of multilayer coverage contain significant intensity near 360 K, which can be attributed to 3D particles formed on the surface at 325 K, and are thermally stable up to the desorption temperature. These observations are consistent with the report of 3D islands of potassium that were found in the same system using XPS measurements.[36(c)]

The second, broader peak around 390 K is essentially identical for initial coverages above 1.3 ML. It represents the maximum SH signal obtained during SH-TPD and it roughly corresponds to the same potassium atom density that is obtained at the maximum signal measured during deposition, as shown in Fig. 3. The 390 K peak is an order of magnitude stronger than the SH response of a multilayer coverage of potassium, represented by the signal seen between 100 and 300 K at coverages above 3 ML (see Fig. 4). The precise origin of this peak is difficult to determine without a structural analysis in this coverage range, by scanning tunneling microscopy (STM), for instance. It is reasonable to suggest, however, that, in analogy to the maximum SH signal seen for alkali metals on metal surfaces mentioned above, this maximum corresponds to a distribution of neutral surface particles where the 2D clusters dominate. On metallic substrates a similar situation occurs just at the completion of the first monolayer. On the chromium oxide surface, the fraction of 2D neutral clusters gradually increases in the coverage range between 1.0 and 2.0 ML, following the completion of the first monolayer, as determined from the TPD and work-function change data discussed in the previous sections. At coverages above 2 ML, 3D islands gradually dominate the surface distribution of particles. The complex dependence of the SH response on the electronic nature of the potassium clusters, and probably also on their size, requires a direct determination of the cluster size distribution by means of, e.g., STM, in order to support the hypothesis discussed above.

D. Diffusion of K on Cr_2O_3(0001)/Cr(110)

A brief review is given here of the most important issues related to grating formation and measuring diffusion via SH diffraction.[11–15] First, a laser beam of intensity I_0 is divided into two beams of intensities rI_0 and $(1-r)I_0$, where r is the splitting ratio between the two components (0.5 in our case). The two beams are directed at an angle of $\pm\phi$ with respect to the surface normal and recombine to form an interference pattern on the surface. This recombination produces a one-dimensionally modulated intensity according to the equation

$$I(x)=I_0+2I_0\sqrt{r(1-r)}\cos(2\pi x/w), \tag{1}$$

where $I(x)$ is the intensity at a point x, w is the grating period $[\lambda/(2\sin\phi)=3.33\,\mu\mathrm{m}]$, λ is the wavelength of the laser light (1.064 μm), and $\phi=\pm 9.2°$. For an incident angle of the probe laser of 44.3°, the first-order diffraction peak should appear at 12.8° from the zero-order beam. Once the light absorption by the chromium substrate is known, the surface temperature along the surface can be calculated. Desorption kinetic parameters of potassium atoms from the chromium oxide were derived from the TPD data discussed above. These were determined as a function of coverage for the first monolayer and then for 2D islands and 3D clusters. Having such information, one can simulate the coverage modulation profile.[15,40(b)] In the particular case of K on Cr_2O_3(0001)/Cr(110), we have shown that the maximum (actually absorbed) laser power used in our experiments for grating formation (11 MW/cm^2) is sufficient to desorb only 3D particles within the TPD peak at 360 K.[45] The periodic coverage modulation thus simulated can be expressed as a Fourier series in coverage,

$$\theta(x)=\theta_0+\sum_{n=1}^{\infty}\Theta_n\cos(2\pi nx/w), \tag{2}$$

where θ_0 is the average surface coverage over a single grating period. Diffraction of the SH signal is obtained due to the periodic modulation obtained in the second-order susceptibility $\chi^{(2)}$.[11–15,30] This modulation need not be identical to the coverage modulation, as is the case here, when the susceptibility is not linearly dependent on coverage due to resonance enhancements as a function of cluster size (see below). Nevertheless, the intensity of the first-order diffraction signal reflects the modulation depth and its decay allows direct monitoring of the coverage profile smearing due to diffusion.

The one-dimensional second Fick's diffusion equation for the simple case where the diffusion rate coefficient is independent of coverage simplifies to

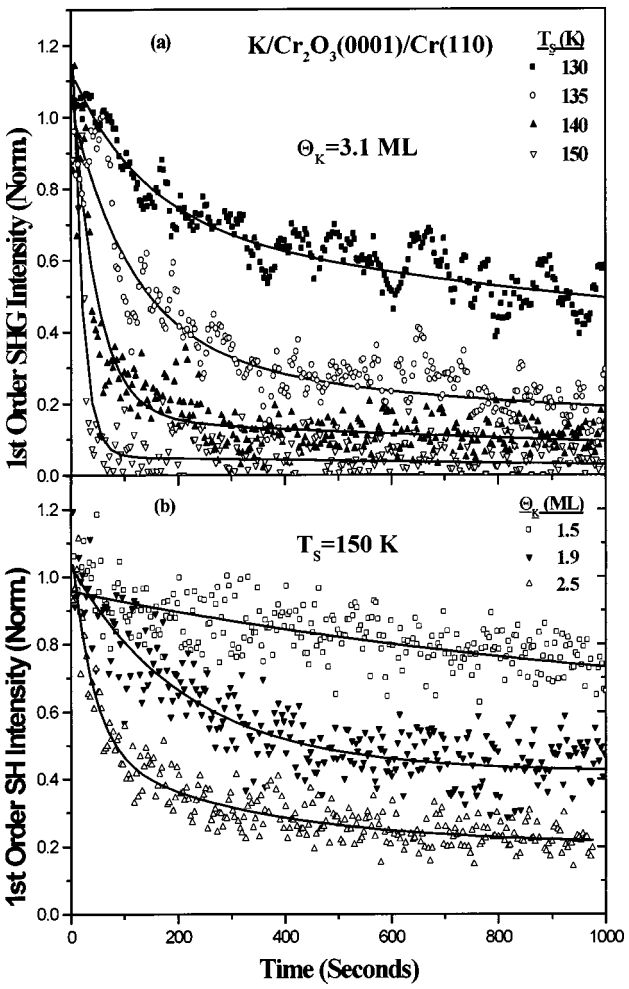

FIG. 5. First-order SH diffracted peak intensity vs time (a) for initial potassium coverage of 3.1 ML at the four indicated surface temperatures and (b) at surface temperature of 150 K for the three indicated initial coverages.

$$\frac{\partial\theta}{\partial t}=D\frac{\partial^2\theta}{\partial x^2}, \tag{3}$$

which has an analytical solution for the coverage $[\theta(x,t)]$ as a function of time. It can be transformed into the following expression for the diffracted SH signal:

$$I_n^{2\omega}(t)\propto(\Theta_n)^2=I_n^{2\omega}(t=0)e^{-8\pi^2n^2Dt/w^2}, \tag{4}$$

where n is the SH diffraction order, Θ_n is the nth-order Fourier component of the coverage modulation, D is the rate constant for diffusion, and w is the coverage modulation period. Fourier transform analysis of the coverage profile generates Fourier components whose magnitudes should be proportional to the square root of the experimental SH diffraction peaks.[11,43] In general, however, the diffusion coefficient is coverage dependent, and therefore the relevant equation should be

$$\frac{\partial\theta(x)}{\partial t}=\frac{\partial}{\partial x}\left(D[\theta(x)]\frac{\partial\theta(x)}{\partial x}\right). \tag{5}$$

In the $K/Cr_2O_3(0001)$ system, we apply the analysis given in Eqs. (3) and (4) by limiting the coverage modulation depth to $\pm10\%$ around an average final coverage [θ_0 in Eq. (2)]. Under these conditions one can approximate the decay of the first-order SH diffraction signal as taking place at a constant coverage and therefore expected to follow an exponential decay.

Decay curves of the first-order SH signal obtained from the potassium grating are shown in Fig. 5 for different surface temperatures [Fig. 5(a)] and for several initial potassium coverages at a fixed surface temperature of 150 K [Fig. 5(b)]. The dependence of the diffusion rate on coverage is seen at coverages in the range 1.5–2.5 ML, where a growing fraction of 3D islands exists on the surface. For each of these initial K coverages, the corresponding Arrhenius plot is shown in Fig. 6. These plots were analyzed on the basis of the rate equation $D=D_0\exp(-E_{\rm diff}/kT)$, where $E_{\rm diff}$ is the activation energy for diffusion and D_0 is the preexponential factor. Finally, both the apparent activation energy for diffusion and the preexponential factor, obtained from Fig. 6, are displayed in Fig. 7 as a function of the initial potassium coverage. The apparent activation energy for diffusion de-

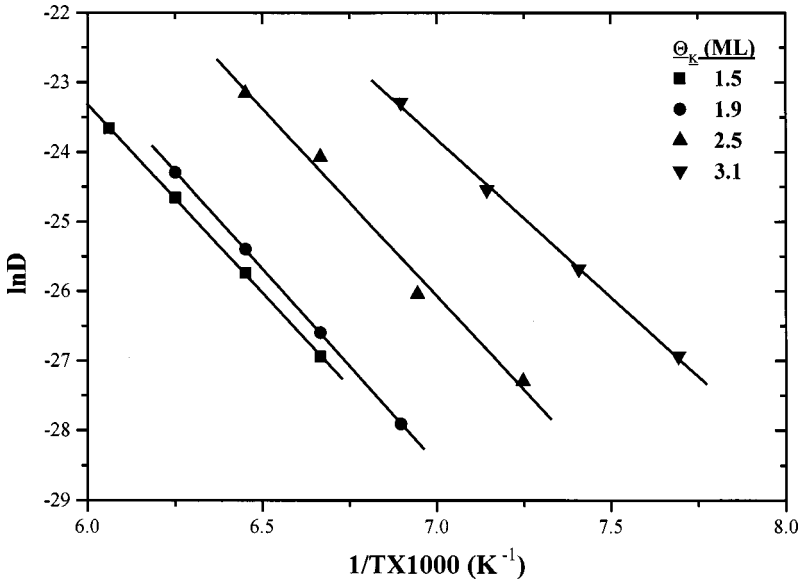

FIG. 6. Arrhenius plots obtained from the curves in Fig. 5 for the indicated initial potassium coverages.

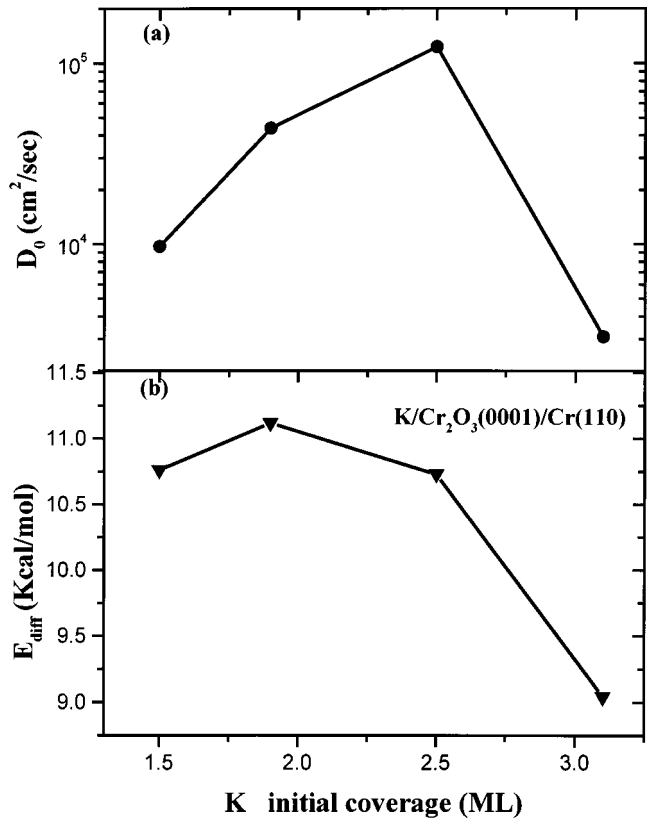

FIG. 7. Activation energy for diffusion (b) and the corresponding preexponential factors (a) as a function of the initial potassium coverage.

picted in Fig. 7 is only marginally dependent on coverage in the range 1.5–2.5 ML. At higher coverages it starts to drop.

The question arises as to what exactly is the diffusion process we follow. It is clear from the laser power used for the grating formation based on LITD that only potassium atoms adsorbed on top of 2D islands (thermally desorbing near 360 K) can be removed using the laser desorption technique, as discussed above.[45] This was verified by comparing potassium TPD following the high-power laser strike to that without the laser heating. Only the 360 K peak was substantially decreased by the LITD method. We create, therefore, a modulated density of 3D particles along the surface while forming the grating. The diffusion process we monitor must reflect the smearing of the density modulation of these 3D clusters.

Two 3D-island migration mechanisms need to be considered. (a) Potassium atoms on top of 2D islands diffuse to the edge of the island and then descend by hopping to the terrace below (first layer of potassium). (b) Complete 3D islands migrate on top of the first highly ionic potassium layer. Both mechanisms lead to a smearing of the originally prepared density modulation of the 3D clusters. It is more likely, we believe, that single atoms on top of the 2D islands diffuse at the relatively low temperatures (130–160 K) at which the surface diffusion/migration occurs in this system. The observed barrier for diffusion of 11 kcal/mol, therefore, should reflect the activation energy for hopping from the 2D islands to the terrace below, considered as a Schwoebel-Ehrlich barrier for a descending step.[46]

The migration of complete 3D islands is less likely to be the migration mechanism. 3D-island migration is expected to be associated with a far larger activation energy for migration, and therefore a much higher onset temperature for such a mechanism is expected. High-temperature STM images of metallic clusters on oxide surfaces have demonstrated the thermal stability of the metallic clusters for several systems.[3,4]

The origin of the change in both the activation energy and the preexponential factor for diffusion seen in Fig. 7 at coverages above 2.5 ML needs to be addressed. One possible explanation, somewhat speculative at this point, is that at coverages above 2.5 ML the density of the 2D islands approaches the percolation threshold. This causes the diffusion rate of third-layer atoms to be determined by migration along 2D terraces rather than by descending barriers, and thus it is expected to be lower, as observed in Fig. 7.

IV. CONCLUSIONS

The interaction and surface diffusion of potassium atoms on the surface of Cr_2O_3(0001)/Cr(110) has been studied using work-function, TPD, and second-harmonic generation measurements. We have found that upon adsorption the potassium atoms tend to form a uniform first layer of partially ionic adsorbed potassium atoms, followed by 2D islands and 3D clusters. These layers are characterized by three distinct desorption peaks near 600 K (first layer), 450 K (2D islands), and 360 K (3D clusters). Work-function change measurements were used to monitor the formation of a potassium oxide surface compound following annealing of the first potassium layer above 580 K for coverages higher than 0.5 ML. The growth of 2D islands was also detected by $\Delta\Phi$ measurements.

The optical SHG signal monitored during the deposition process goes through a maximum at potassium coverage near 1.4 ML, supporting the observation of island formation in the second layer. Recording the SHG signal during surface heating in the SH-TPD mode, we can clearly distinguish between the first potassium layer, 2D islands, and 3D clusters, each represented by separate peaks.

The diffusion of metal atoms on the surface of an oxide is reported here, achieved using optical SH diffraction from a laser-induced desorption coverage grating. A coverage-independent activation energy for surface diffusion of 11 kcal/mol has been determined in the coverage range of 1.2–2.5 ML. The activation energy dropped to 9 kcal/mol as the coverage increased to 3.0 ML. We conclude that the diffusion process is most likely described by the mobility of potassium atoms on top of second-layer 2D islands. The experimentally observed barrier for diffusion, therefore, should reflect the activation energy for descending from the 2D islands to the first-layer potassium terrace below, the so-called Scwoebel-Ehrlich barrier.

ACKNOWLEDGMENTS

This work was partially supported by the Israel Science Foundation and the German Israeli Foundation. The Farkas Research Center for Light Induced Processes is supported by the Minerva Gesellschaft für die Forschung, GmbH, München.

*Corresponding author.
[1] C. Noguera, *Physics and Chemistry at Oxide Surfaces* (Cambridge University Press, Cambridge, 1996).
[2] S. C. Street, C. Xu, and D. W. Goodman, Annu. Rev. Phys. Chem. **48**, 43 (1997).
[3] H. J. Freund, Angew. Chem. Int. Ed. Engl. **36**, 452 (1997).
[4] C. T. Campbell, Surf. Sci. Rep. **27**, 1 (1997).
[5] M. Valden, X. Lai, and D. W. Goodman, Science **281**, 1647 (1998); M. Valden and D. W. Goodman, Isr. J. Chem. **38**, 285 (1999).
[6] A. G. Naumovets and Yu. S. Vedula, Surf. Sci. Rep. **4**, 365 (1984).
[7] R. Gomer, Rep. Prog. Phys. **53**, 917 (1990).
[8] *Laser Spectroscopy and Photochemistry on Metal Surfaces, Parts I and II*, edited by H.-L. Dai and W. Ho (World Scientific, New York, 1995).
[9] A. A. Deckert, J. L. Brand, M. V. Arena, and S. M. George, Surf. Sci. **208**, 441 (1989).
[10] E. D. Westre, D. E. Brown, J. Kutzner, and S. M. George, Surf. Sci. **294**, 185 (1993).
[11] X.-D. Xiao, X. D. Zhu, W. Daum, and Y. R. Shen, Phys. Rev. B **46**, 9732 (1992).
[12] X.-D. Xiao, X. D. Zhu, W. Daum, and Y. R. Shen, Phys. Rev. B **48**, 17 452 (1993).
[13] G. A. Reider, U. Höfer, and T. F. Heinz, Phys. Rev. Lett. **66**, 1994 (1991).
[14] X. D. Zhu, A. Lee, A. Wong, and U. Linke, Phys. Rev. Lett. **68**, 1862 (1992).
[15] Z. Rosenzweig, I. Farbman, and M. Asscher, J. Chem. Phys. **98**, 8277 (1993).
[16] B. Bayat and H.-W. Wassmuth, Surf. Sci. **133**, 1 (1983).
[17] M. Šnábl, M. Ondrejcek, V. Cháb, W. Stenzel, H. Conrad, and A. M. Bradshaw, Surf. Sci. **352–354**, 546 (1996).
[18] J. Ellis and J. P. Toennies, Phys. Rev. Lett. **70**, 2118 (1993).
[19] M. Ondrejcek, W. Stenzel, H. Conrad, V. Cháb, Z. Chvoj, W. Engel, and A. M. Bradshaw, Chem. Phys. Lett. **215**, 528 (1993).
[20] E. D. Westre, D. E. Brown, J. Kutzner, and S. M. George, J. Chem. Phys. **104**, 7313 (1996).
[21] L. Schmidt and R. Gomer, J. Chem. Phys. **42**, 3573 (1965).
[22] J. Neugebauer and M. Scheffler, Phys. Rev. Lett. **71**, 577 (1993).
[23] S. Modesti, C. T. Chen, Y. Ma, G. Meios, P. Rudolf, and F. Setter, Phys. Rev. B **42**, 5381 (1990).
[24] J. N. Andersen, E. Lundgren, R. Nyholm, and M. Qvarford, Surf. Sci. **289**, 307 (1993).
[25] E. Lundgren, A. Beutler, R. Nyholm, J. N. Andersen, and D. Heskett, Surf. Sci. **370**, 311 (1997).
[26] T. Artuga, H. Tochiara, and Y. Murata, Surf. Sci. **158**, 490 (1985).
[27] R. H. Bergmans, A. L. G. P. Brands, A. W. Denier van der Gon, W. C. A. N. Ceelen, H. H. Brongersma, P. Bielen, and C. Creemers, Surf. Sci. **350**, 1 (1996).
[28] D. L. Adams, Appl. Phys. A: Mater. Sci. Process. **62**, 123 (1996).
[29] S. V. Christensen, J. Nerlov, K. Nielsen, J. Burchhardt, M. M. Nielsen, and D. L. Adams, Phys. Rev. Lett. **76**, 1892 (1996).
[30] (a) W. Zhao, R. W. Verhoef, and M. Asscher, J. Chem. Phys. **107**, 5554 (1997), (b) G. Kerner and M. Asscher (unpublished).
[31] X. D. Zhu, Th. Rasing, and Y. R. Shen, Phys. Rev. Lett. **61**, 2883 (1988).
[32] G. A. Reider, M. Huemer, and A. J. Schmidt, Opt. Commun. **68**, 149 (1988).
[33] X.-D. Xiao, Y. Xie, and Y. R. Shen, Surf. Sci. **271**, 295 (1992).
[34] X. D. Zhu, A. Lee, and A. Wong, Appl. Phys. A: Solids Surf. **52**, 317 (1991)
[35] X. D. Zhu, Mod. Phys. Lett. B **6**, 1217 (1992).
[36] (a) B. Dillmann, F. Rohr, O. Seiferth, G. Klivenyi, M. Bender, K. Homann, I. N. Yakovkin, D. Ehrlich, M. Baumer, H. Kuhlenbeck, and H.-J. Freund, Faraday Discuss. **105**, 295 (1996); (b) M. Wilde, I. Beauport, K. Al-Shamery, and H.-J. Freund, Surf. Sci. **390**, 186 (1997); (c) M. Wilde, I. Beauport, F. Stuhl, K. Al-Shamery, and H.-J. Freund, Phys. Rev. B **59**, 13 401 (1999); (d) F. Rohr, M. Bäumer, H.-J. Freund, J. A. Mejias, V. Staemmler, S. Müller, L. Hammer, and K. Heinz, Surf. Sci. **372**, L291 (1997).
[37] Z. Rosenzweig and M. Asscher, J. Chem. Phys. **96**, 4040 (1992).
[38] Z. Rosenzweig and M. Asscher, in *Surface Science of Catalysis*, ACS Symposium Series No. 482, edited by D. J. Dwyer and F. M. Hoffman (American Chemical Society, Washington, DC, 1992).
[39] T. Livneh and M. Asscher, J. Phys. Chem. B **101**, 5705 (1997).
[40] (a) *Physics and Chemistry of Alkali Metal Adsorption*, Vol. 57 of *Materials Science Monographs*, edited by H. P. Bonzel, A. M. Bradshaw, and G. Ertl (Elsevier Amsterdam, 1989); (b) R. W. Verhoef, W. Zhao, and M. Asscher, J. Chem. Phys. **106**, 9353 (1997), and references therein; (c) K. J. Song, D. Heskett, H. L. Dai, A. Liebsch, and E. W. Plummer, Phys. Rev. Lett. **61**, 1380 (1988).
[41] R. W. Verhoef and M. Asscher, Surf. Sci. **391**, 11 (1997).
[42] A. J. Topping, Proc. R. Soc. London, Ser. A **114**, 67 (1927).
[43] J. Neugebauer and M. Scheffler, Phys. Rev. Lett. **71**, 577 (1993).
[44] H. W. K. Tom, C. M. Mate, X. D. Zhu, J. E. Crowell, Y. R. Shen, and G. A. Somorjai, Surf. Sci. **172**, 466 (1986).
[45] K. Prabhakaran, D. Purdie, R. Casanova, C. A. Muryn, P. J. Hardman, P. L. Wincott, and G. Thornton, Phys. Rev. B **45**, 6969 (1992).
[46] G. Ehrlich, Appl. Phys. A: Solids Surf. **55**, 403 (1992); Surf. Sci. **331**, 403 (1995).